Inelastic collisions of solitary waves in anisotropic Bose–Einstein condensates: sling-shot events and expanding collision bubbles



2013 New J. Phys. 15 113028

(http://iopscience.iop.org/1367-2630/15/11/113028)

New Journal of Physics
The open access journal for physics

# Inelastic collisions of solitary waves in anisotropic Bose–Einstein condensates: sling-shot events and expanding collision bubbles

**C Becker[1], K Sengstock[1], P Schmelcher[2], P G Kevrekidis[3] and R Carretero-González[4,5]**

[1] Institut für Laser-Physik, Universität Hamburg, Luruper Chaussee 149, D-22761 Hamburg, Germany
[2] Zentrum für Optische Quantentechnologien, Universität Hamburg, Luruper Chaussee 149, D-22761 Hamburg, Germany
[3] Department of Mathematics and Statistics, University of Massachusetts, Amherst, MA 01003-4515, USA
[4] Nonlinear Dynamical Systems Group, Computational Science Research Center, and Department of Mathematics and Statistics, San Diego State University, San Diego, CA 92182-7720, USA
E-mail: rcarretero@mail.sdsu.edu

*New Journal of Physics* **15** (2013) 113028 (17pp)
Received 14 August 2013
Published 13 November 2013
Online at http://www.njp.org/
doi:10.1088/1367-2630/15/11/113028

**Abstract.** We study experimentally and theoretically the dynamics of apparent dark soliton stripes in an elongated Bose–Einstein condensate. We show that for the trapping strengths corresponding to our experimental setup, the transverse confinement along one of the tight directions is not strong enough to arrest the formation of solitonic vortices or vortex rings. These solitonic vortices and vortex rings, when integrated along the transverse direction, appear as dark soliton stripes along the longitudinal direction thereby hiding their true character. The latter significantly modifies the interaction dynamics during collision events and can lead to apparent examples of inelasticity and what may appear experimentally even as a merger of two dark soliton stripes. We explain this feature by means of the interaction of two solitonic vortices leading to a sling shot event with one of the solitonic vortices being ejected at a relatively

[5] Author to whom any correspondence should be addressed.

large speed. Furthermore we observe expanding collision bubbles which consist of repeated inelastic collisions of a dark soliton stripe pair with an *increasing* time interval between collisions.

## Contents



## 1. Introduction

Over the past 15 years, the advent of Bose–Einstein condensates (BECs) has created unprecedented possibilities for the examination of phenomena involving nonlinear waves [1, 2]. Ranging from bright solitary waves [3–5] and gap matter waves [6] to excitations of defocusing (repulsively interacting) media most notably dark solitons [7, 8], vortices [7, 9, 10], as well as solitonic vortices and vortex rings [11, 12], the exploration of these phenomena has attracted considerable theoretical as well as experimental interest.

Early experiments on dark solitons [13–16] were, at least in part, limited by the lifetimes of these states under the influence of dynamical instabilities in higher dimensional settings or the effect of thermal fluctuations at temperatures closer to the transition temperature. Nevertheless, more recent experiments have been able to produce a significantly increased experimental control [17–22]. The resulting combination of sufficiently low temperatures with—in some of the cases—more quasi-one-dimensional (1D) regimes has led to clear-cut observations of oscillating and interacting dark solitons, bearing good agreement with theoretical predictions for these structures.

Vortices, in turn, constitute the quasi-two-dimensional (2D) generalization of dark solitons. Following a ground breaking experiment where vortices were produced using a phase-imprinting method [23], other experiments produced these structures by using a phase-imprinting method between two hyperfine spin states of a $^{87}$Rb BEC [24], or by stirring of the BECs [25] above a certain critical angular speed [26–29]. This led to the production of few vortices [29] and even of very robust vortex lattices [30]. Such states were also produced by other methods including dragging obstacles through the BEC [31, 32], the nonlinear interference of condensate fragments [33], or even the use of the Kibble–Zurek mechanism [34, 35]. Vortices of higher charge were also produced and their dynamical instability was considered [36].

The three-dimensional (3D) generalization of the above states consists of multiple possibilities. The most prominent among them are solitonic vortices (or vortex lines) and vortex rings [7, 12], both of which emerge from the instability of the dark soliton stripe—the multi-dimensional analogue of a 1D dark soliton [37]. A solitonic vortex is the 3D extension of a 2D vortex by (infinitely and homogeneously) extending the solution into the axis perpendicular to the vortex plane. In a realistic experimental setup, which requires an external trapping potential,

the solitonic vortices naturally acquire a finite length. In that case, solitonic vortices are vorticity 'tubes' that are straight across the BEC cloud or bent in U or S shapes depending on the aspect ratio of the BEC cloud [38, 39]. If a solitonic vortex is bent enough to close on itself or if two solitonic vortices are close enough to each other they can produce a vortex ring [40]. Vortex rings are 3D structures whose core is a closed loop with vorticity around it [41] (i.e. a vortex that is looped back into itself). Vortex rings can also be produced by an impurity traveling faster than the speed of sound of the background [42]; by nonlinear interference between colliding blobs of the background material [43, 44]; by phase and density engineering techniques [22, 45]; or even by introducing 'bubbles' of one component in the other component in two-component BEC systems [46].

In the present work we show how in experimentally available settings it is possible to produce an interplay between 1D and 3D phenomenologies (with the 2D case, as an interesting intermediary—see below). This regime is related to the one presented in [47] where hybrid solutions comprising of dark soliton shells and vortex rings were observed. In our work, we explore further the interplay between dimensionalities and use some complement of the data of the experiments in [18, 19] that was previously unexplained. In particular, we show how this interplay is found to be responsible for *dramatic* events such as seemingly perfectly 'plastic' collisions (which entirely defy the near-integrable nature of solitary waves as such). We show that such events which we have observed in our experiments are not aberrations but rather a direct consequence of the hidden character of the solitons, namely their conversion to solitonic vortices during their dynamical evolution. The strong interaction of such solitonic vortices is found to potentially sling shot one of them toward the background and produce such a 'plastic' collision which appears as a merger of two dark soliton stripes when integrated along one spatial dimension—as it necessarily happens in absorption imaging in current experimental settings. Further counter-intuitive phenomena occurring in this setup include a sequence of apparent dark soliton stripe collisions with increasing collision times, i.e. a series of 'expanding collision bubbles'. This is shown to be produced by mutual rotation of solitonic vortices around each other.

Our presentation is structured as follows. In section 2 we present the experimental setup and the corresponding experimental observations displaying the apparent, unexpected, merger of two dark soliton stripes. In section 3 we introduce the theoretical model and its corresponding numerical experiments that allow to elucidate the nature of this unexpected merger. We also include in this section some other intriguing cases where solitonic vortices rotating around each other tend to slow down their rotation frequency. Finally, in section 4 we present our conclusions and identify some future areas for possible exploration.

## 2. Experimental setup and observations

For the experiments presented here we start by trapping $5 \times 10^9$ atoms of $^{87}$Rb in a magneto-optical trap which are subsequently compressed and cooled in an optical molasses. The atoms are further cooled by evaporative cooling in a magnetic trap before we load them into an optical dipole trap. After a second evaporative cooling stage over 20 s, an elongated and almost pure BEC of about $5 \times 10^4$ atoms in the $|5^2S_{1/2}, F = 1, m_F = -1\rangle$ state is produced with a chemical potential of less than 20 nK. The trap frequencies read $\omega_{x,y,z} = 2\pi \times (85, 133, 5.9)$ Hz (and are known within an accuracy of $\pm 2$–$3\%$). These correspond to a 'cigar-shaped' trap elongated along the $z$-direction and strongly confined along the transverse $x$ and $y$ directions. The peak

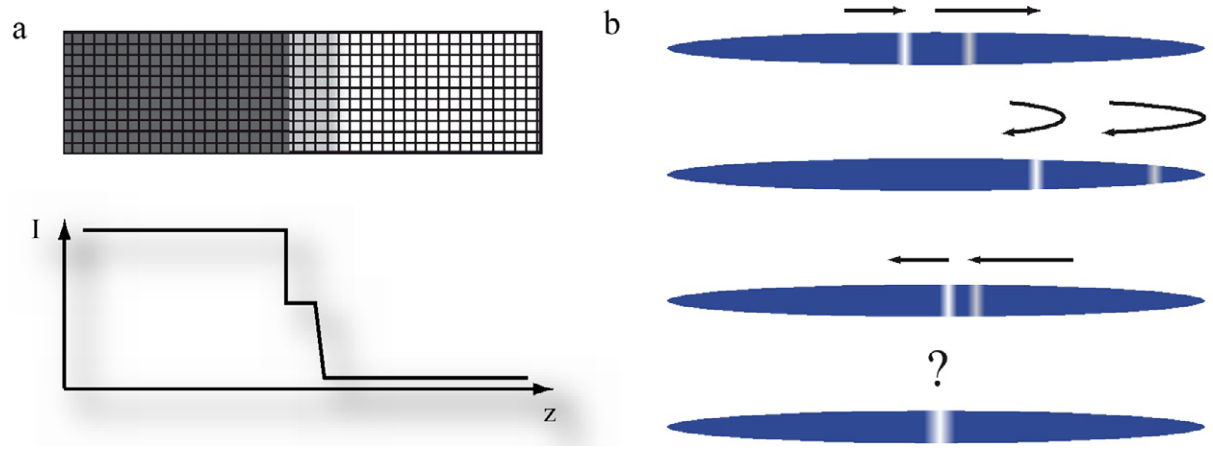


**Figure 1.** Experimental setup for the chase scenario for two dark soliton stripes. Two dark soliton stripes are generated that travel in the same direction at different velocities. After a quarter oscillation period they reverse their direction of propagation and travel in the opposite direction where the fast soliton will eventually overtake its slower counterpart. (a) Intensity profile used to generate two solitons at different velocities. To generate a faster soliton less phase feed is applied over a larger region. (b) Schematic representation of the chase scenario of a fast (indicated by a gray stripe) and a slow (indicated by a white stripe) soliton.

density of $n_0 = 5.8 \times 10^{13}\,\mathrm{cm}^{-3}$ corresponds to a speed of sound of $c_s = 1.0\,\mathrm{mm\,s}^{-1}$ and a healing length of $\xi = 0.7\,\mu\mathrm{m}$.

In order to seed dark soliton stripe structures in the experiment, we employ the well-established method of optical phase imprinting in Bose–Einstein condensates [13, 14, 18]. For this purpose a laser pulse of 70 $\mu$s duration, blue-detuned from atomic resonance by 8 GHz is used. We create almost arbitrary intensity patterns employing a spatial light modulator and image those patterns onto the BEC through a high quality objective yielding an optical resolution of better than 2 $\mu$m. In this way, the number of dark soliton stripes created can be varied, as can their individual depths, initial positions and directions of movement be chosen over a wide range of parameters by tailoring the light field potentials acting on the BEC accordingly. For the experiment described here, we image a two-step intensity profile (see figure 1(a)) onto the BEC, thus creating one dark soliton stripe at each phase jump. After a certain evolution time we switch off the trapping potential and allow the condensate to freely expand for a time-of-flight of 11.5 ms before we image the condensates employing on-resonance absorption imaging. The optical resolution of our imaging lens is slightly better than 2 $\mu$m and the expansion time leads to greatly enhanced visibility of the solitons whose width in the trap is on the order of the healing length (700–900 nm) only. Particle number fluctuations are below 10% from shot-to-shot in our experiments.

As schematically depicted in figure 1(b), two dark soliton stripes are generated in that way which travel in the same direction at different velocities. The shallower and thus faster soliton starts ahead of the deeper and slower soliton. After a quarter oscillation period the solitons reverse their direction of propagation and travel in the opposite direction where the fast soliton will eventually overtake its slower counterpart. The solitons start approximately

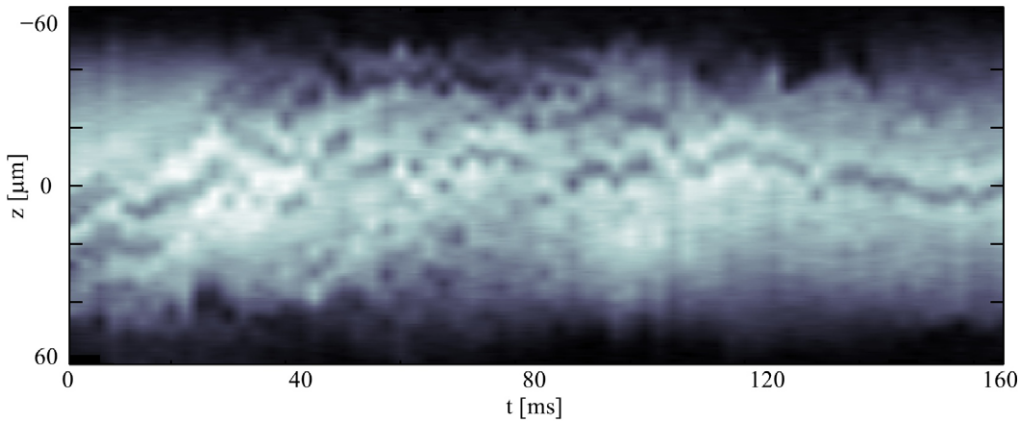


**Figure 2.** Experimental results depicting the chasing scenario between two dark soliton stripes. Shown is the density plot of the condensate. Each column represents the optical density of the elongated condensate integrated along the transverse directions. The density depressions of the apparent dark soliton stripes as well as the increased density of the density waves are clearly visible. While it cannot be deduced what exactly happens during the collision, it is clearly seen that for long evolution times a single very deep soliton that hardly moves at all is formed. Note that we have observed structures similar to the last 45 ms of the graph for evolution times up to 5 s!.

20 $\mu$m apart from each other, the fast advancing soliton with a measured initial speed of $\dot{q}_0^{\mathrm{f}} = 0.7\,\bar{c}_{\mathrm{s}}$ and the slower soliton traveling at $\dot{q}_0^{\mathrm{s}} = 0.62\,\bar{c}_{\mathrm{s}}$. According to nonlinear Schrödinger theory these values would correspond to depths of $n_{\mathrm{s}}^{\mathrm{f}}/n_0 = 0.51$ and $n_{\mathrm{s}}^{\mathrm{s}}/n_0 = 0.61$ respectively. The associated phase slips across the nodal planes of the solitons read $\Delta\phi^{\mathrm{f}} = 0.50\pi$ and $\Delta\phi^{\mathrm{s}} = 0.57\pi$ for the fast and slow soliton respectively.

Figure 2 shows the experimental results of the time-evolution of two dark soliton stripes created according to the above-mentioned experimental conditions. For each experiment the system was let to evolve for a predetermined amount of time and then imaged. A total of more than 60 images were extracted 2.5 ms apart from each other. Each image was then integrated along the remaining transverse direction to obtain the (integrated) 1D density along the, longitudinal, $z$ direction. Finally, the overall evolution of the effective 1D system is rendered visible by plotting these densities as columns in figure 2. In the figure it is possible to see the two initial two dark soliton stripes that travel toward the center of the trap. Note that additional excitations of the condensate generated during the phase imprinting process are significantly damped prior to the soliton interaction which ensures a better visibility of the collision process. After the dark soliton stripes bounce back from the opposite edge of the cloud, they strongly interact and *apparently merge* after some 100 ms. Although the variation from one experiment to the next does not allow for a clear depiction of the dynamics during the collision process, we systematically obtained a resulting cloud with a single apparent dark soliton stripes in it. This attests to the robustness of the process.

After closer inspection of the individual snapshots, before integration about the transverse direction, it is evident that the dynamics is not only governed by dark soliton stripes. This is due to the fact that the dark soliton stripes tend to bend and decay into vortex rings [48] and also

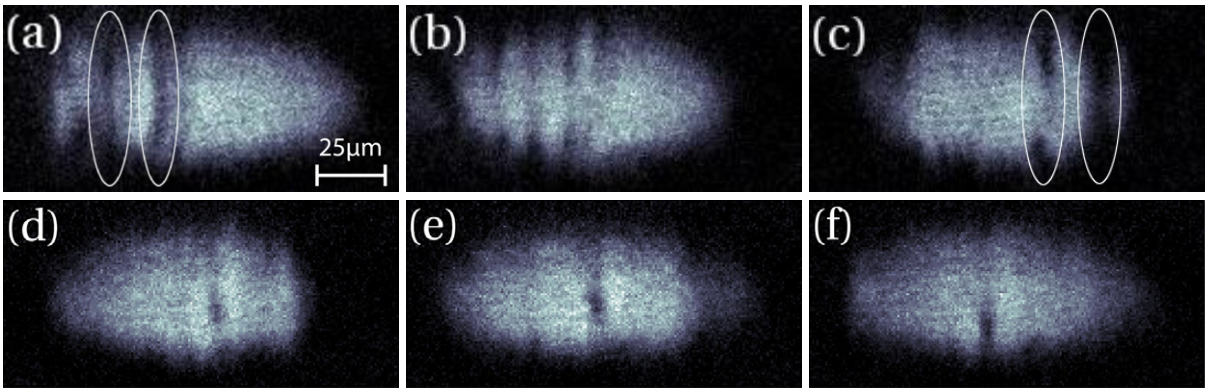


**Figure 3.** Samples of individual snapshots that make up the dynamics depicted in figure 2. The different panels correspond to times $t =$ (0, 12, 57, 119, 136, 155) ms. (a) Initial state containing two dark soliton stripes. The ruler corresponds to the in-trap size of the condensate prior to time-of-flight. (b) The dark soliton stripes decay into vortex rings. (c) The solitons reach the opposite edge of the cloud and bounce back. (d)–(f) After the strong interaction a single, stable, solitonic vortex is left in the system.

periodically oscillate between dark soliton stripes and vortex rings [22]. This behavior can be seen in the experimental snapshots depicted in figure 3. In particular, the first row of snapshots corresponds to two initial dark soliton stripes that start bending (see dark lines inside the ellipses in panel (a)) and decay into vortex rings (panel (b)). As the vortex rings approach the opposite edge of the trap they recombine into a dark soliton stripe due to the strong confinement of the trap's edge (see dark soliton stripe very close to the right edge inside the right-most ellipse in panel (c)). After the 'merger' between the two solitons a single solitonic vortex remains in the cloud performing oscillations back and forth along the longitudinal direction (see panels (d)–(f)).

## 3. Model and numerical observations

In an attempt to better understand the dynamics seen in the experiments we model the BEC cloud using realistic parameter values and initial conditions. For this we use the 3D Gross–Pitaevskii (GP) equation that has been shown to accurately describe the mean-field dynamics of the BEC for low enough temperatures and large enough particle numbers, as is the case for our setting. The GP equation, in three dimensions, for the wavefunction $\psi(x, y, z, t)$ takes the form

$$\mathrm{i}\hbar\frac{\partial\psi}{\partial t} = \left[-\frac{\hbar^2}{2m}\nabla^2 + V(r) + g_{3\mathrm{D}}|\psi|^2\right]\psi, \tag{1}$$

where $\nabla^2$ is the 3D Laplacian, while the trapping potential is given by $V(r) = \frac{1}{2}m(\omega_x^2x^2 + \omega_y^2y^2 + \omega_z^2z^2)$, $m$ is the atomic mass and $\omega_i$ are the trapping frequencies (strengths) along the different directions. The effective nonlinearity strength is given by $g_{3\mathrm{D}} = 4\pi\hbar^2a/m$, with $a$ being the s-wave scattering length. The numerical results presented herein were obtained using second order finite differencing in space and fourth order Runge–Kutta integration in time

for the parameters corresponding to the actual experiment. Specifically, we used a harmonic trapping potential with frequencies (strengths) $\omega_{x,y,z} = 2\pi \times (85, 133, 5.9)$ Hz, $8.7 \times 10^4$ $^{87}$Rb atoms, and a scattering length of 53.37 Å. In what follows, we will consider different initial conditions involving initializing first a single dark soliton stripe and subsequently a few prototypical cases corresponding to two initial dark soliton stripes. For both of these situations we show, as a central result, that the quasi-1D evolution will prove to be somewhat misleading when observed as such. In all cases, it is the true 3D dynamics (and multiple cross-sections of the BEC) that will enable a fundamental understanding of the observations, even when they appear entirely counter-intuitive, at first sight, as is the case with 'plastic' collisions.

The first thing to note about dark soliton stripes in this trapping is that they are *not* always stable; see, e.g. the discussion of [8] and references therein. This instability against transverse long-wavelength perturbations was first identified in the context of nonlinear optics [49–51], where it was also experimentally observed [52–54]. While in a nearly spherical trap considered earlier [8, 55], a dark soliton stripe was shown to decay into vortex rings, in our elongated trap experimental setup, a stationary dark soliton stripe at the center of the trap destabilizes, due to snaking instability, and decays into solitonic vortices (see e.g. [56]). The decay of the dark soliton stripe can be avoided if the transverse direction (length of the dark soliton stripe) is tight enough [57]. In fact, the parameter $\gamma = n_0 g_{3D}/(\hbar\omega_\rho)$, given by the ratio of the mean-field interaction energy at maximum density $n_0$ to the harmonic oscillator energy in the transverse direction [$\omega_\rho = (\omega_x, \omega_y)$], controls the stability of the dark soliton stripe. Specifically, it was shown in [57] that, in a cylindrical trap ($\omega_\rho = \omega_x = \omega_y$), if $\gamma > \gamma_c$ where $\gamma_c \approx 2.4$ for $\omega_\rho \gg \omega_z$, the dark soliton becomes unstable and decays to a solitonic vortex. Our setup is not strictly cylindrical, nonetheless computing the coefficient $\gamma$ for $\omega_\rho = \omega_x$ and $\omega_y$ gives, respectively, $\gamma = 5.3$ and 3.4. This is a clear indication that, in our setup, we are above the $\gamma = \gamma_c$ threshold in both directions and thus there is the possibility for the dark soliton stripe to decay into a solitonic vortex. It should be noted that since the trapping in the $x$-direction ($\omega_x = 2\pi \times 85$) is weaker than the one in the $y$-direction ($\omega_y = 2\pi \times 133$), it is expected that the dark soliton stripe will decay in the $x$-direction giving rise to a solitonic vortex aligned in the $y$-direction. The left panel of figure 4 depicts a numerical example of the evolution ($0 < t < 200$ ms) of this instability in a manner akin to what we have observed in our experiment (cf figure 2). This numerical example suggests that the initial, stationary, dark soliton stripe at the center of the trap apparently breaks into three dark soliton stripes which oscillate and interact. This would obviously be a contradiction for an angular momentum conserving (isotropic) system since any solitonic vortices have to be nucleated in pairs of opposite charge so that total angular momentum remains constant (equal to zero). However, it is important to note that our system is not isotropic and therefore conservation of angular momentum is not applicable here. Therefore, solitonic vortex charge is not conserved—for example, a dark soliton stripe with net solitonic vortex charge of zero can indeed decay into a single solitonic vortex in a non-isotropic setting, as was demonstrated for a cigar-shaped trap in [56]. This also points out that in the presence of anisotropy, there might be some internal structure of the created nonlinear waves that the integrated density picture is failing to capture (see below).

To elucidate the true dynamics of the system it is necessary to analyze the full 3D extent of the condensate. To that effect we will also depict 3D isocontours of density and vorticity of the condensate wavefunction $\psi = |\psi| \exp(\mathrm{i}\,\theta)$. The density corresponds to $|\psi|^2$ while the vorticity corresponds to the curl of the fluid velocity $\vec{v} = \nabla\theta$, which in turn is defined as the gradient of

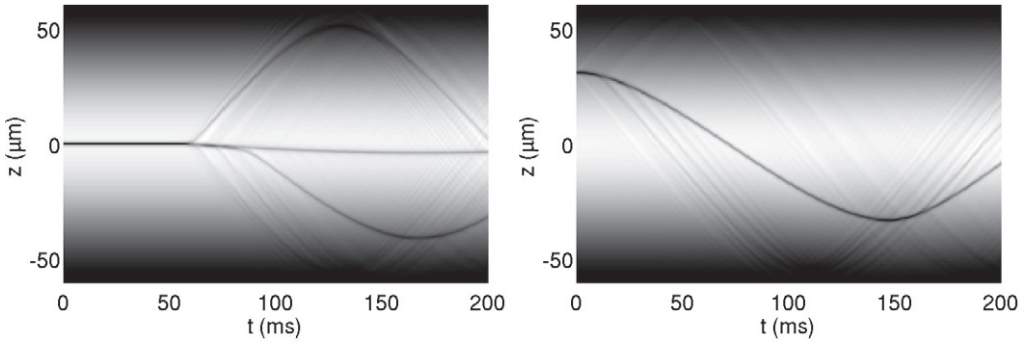


**Figure 4.** Left panel: evolution of an initially stationary dark soliton stripe at the center of the trap. The initial stationary dark soliton stripe solution is obtained by a fixed point iterative technique (Newton method) and it is initially perturbed with a small amount of random white noise. The dark soliton stripe seems to split into three solitons due to its (snaking) instability. Right panel: evolution of dark soliton stripes seeded off center. The initial positions of the soliton is $(1/2)R_{\mathrm{TF}}$ (where $R_{\mathrm{TF}}$ is the Thomas–Fermi radius (half width of) of the cloud). This solitary wave seems to perform stable oscillations along the longitudinal (weak) trap direction. All panels depict the time evolution of the density integrated along the $x$ and $y$ directions in a manner akin to what is done for the experimental results of figure 2.

the phase of the condensate. It is straightforward to show that the fluid velocity is equivalent to

$$\vec{v} = \nabla\theta = \frac{\mathrm{i}}{2}\frac{\psi\nabla\psi^* - \psi^*\nabla\psi}{|\psi|^2}, \tag{2}$$

where $(\cdot)^*$ stands for complex conjugation. It is important to note that the density at the vortex ring core is zero and thus the fluid velocity and the vorticity have a singularity there. To numerically alleviate this issue, we opt to add a small regularizing density factor $\delta$ to the denominator in equation (2). In particular, we use $|\psi|^2 + \delta$ with $\delta = 0.05$ in the denominator of equation (2) which results in two beneficial effects: (i) a finite vorticity at the core and (ii) a smoothing effect of the vorticity that allows the visualization of vorticity isocontours (as demonstrated below).

Figure 5 depicts snapshots, at different times, of density and vorticity isocontours corresponding to the examples depicted in figure 4. As it can be observed from panel (a), it is clear that only *two* solitonic vortices are created. This solitonic vortex pair corresponds to the decay of a vortex ring ($t = 58$ ms) into a solitonic vortex pair ($t = 75$ ms) consisting of two oppositely charged solitonic vortices. Upon closer inspection, the apparent third solitonic vortex that is emitted toward $z > 0$ is actually a weak vortex ring at the periphery of the cloud. This vortex ring is clearly visible at $t = 75$, 100 and 150 ms where it is depicted by the light vorticity isocontours. This vortex ring is the culprit for the 'pinching' of the BEC density at the $z$ coordinate where it lives and thus appears as being on the same footing as the other two solitonic vortices in the integrated density depicted in figure 4. For longer times (data not shown here) the 'collisions' between the two solitonic vortices are fairly elastic since they never get too close to each other (one solitonic vortex remains close to the center of the trap while the other

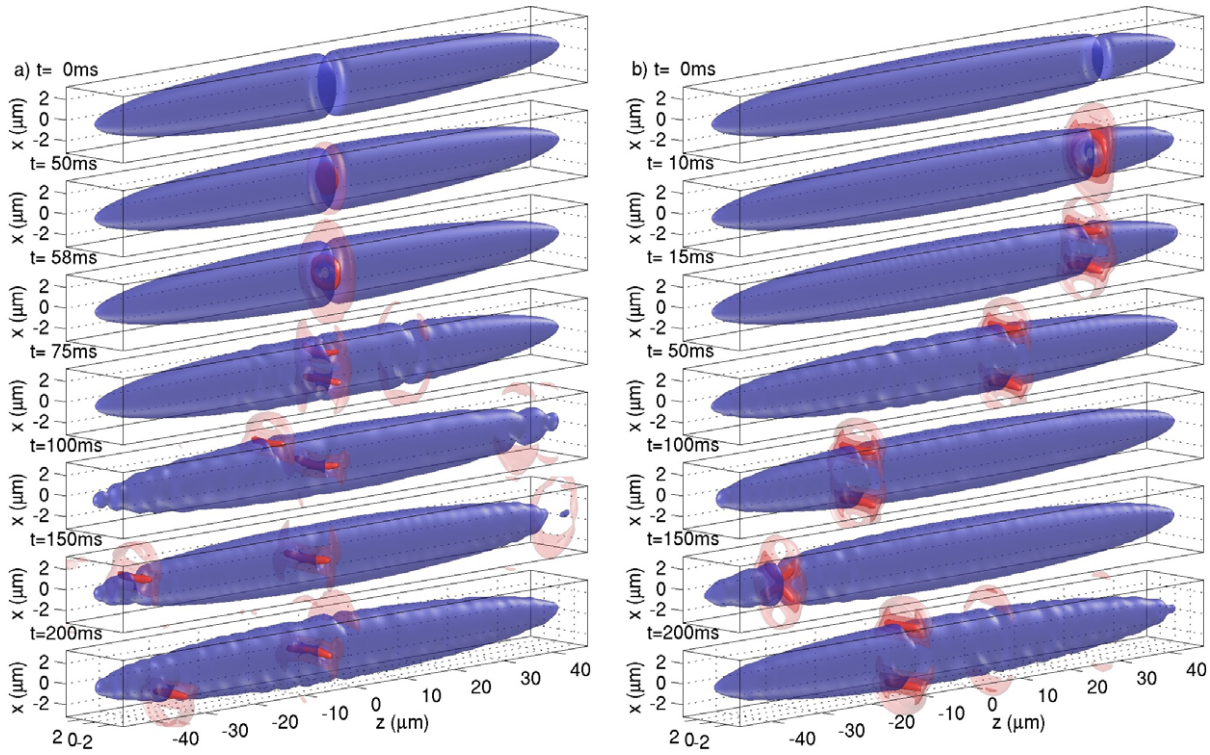


**Figure 5.** 3D renderings corresponding to the numerics shown in figure 4 at the times indicated. The blue background surface corresponds to a density isocontour plot at 40% of the maximum density while the red surfaces correspond to vorticity isocontours. (a) Isocontours at 50% (light) and 85% (solid) of maximum vorticity. (b) isocontours at 50% (very light), 65% (light) and 85% (solid) of maximum vorticity.

one circles the periphery periodically), cf the (asymmetric) profile of an intermediate speed solitonic vortex in figure 3 of [37]. It is important to note that the spatial extent in the $y$ direction is too tight to allow the coherent structure to develop any strong excitation (or instability) in that direction in a manner akin to the arrest of snaking instability shown in [58]. In contrast, the confinement along the $x$-direction is weak enough to allow for the nucleation of solitonic vortices.

We now consider the case of moving dark soliton stripes. When the dark soliton stripes are set in motion, their instability is reduced [59]. We can see this effect in the right panel of figure 4 where a dark soliton stripe with zero initial velocity is placed a certain distance away from the center of the trap. As the panel shows, the dark soliton stripe placed away from the center oscillates back and forth along the $z$ direction of the trap and thus its instability against transverse perturbations is reduced. This is what is also expected based on the transition from absolute to convective instability, as was recently discussed, e.g. in [60]. The specific example depicted in the right panel of figure 4 corresponds to a dark soliton stripe that is initially sufficiently far away from the center ($(1/2)R_{\rm TF}$ away) that it apparently does not split. It should also be noted that this is in line with the observation of, e.g. figure 4 of [37] which suggests that when the speeds are sufficiently large (due to the large initial potential energy

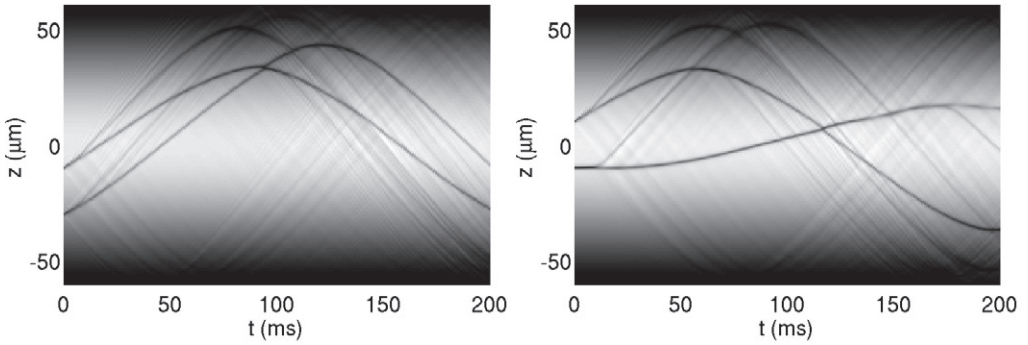


**Figure 6.** Evolution of two colliding dark soliton stripes. Left: collision when a faster dark soliton stripe catches up with a slower one. Right: head on collision of a faster dark soliton stripe that bounces back from condensate edge and collides with a slower moving dark soliton stripe. The dark soliton stripes are indeed solitonic vortex pairs (see figure 7). All panels depict the time evolution of the density integrated about the $x$ and $y$ directions.

in the trap), the soliton and the solitonic vortex merge and are indeed stabilized against the transverse modulations. Nonetheless, the actual dynamics for the evolution of this configuration is not fully revealed until it is depicted in 3D; see panel (b) of figure 5. As it can be observed, the dark soliton stripe decays indeed into a vortex ring ($t = 10$ ms) but it then, in turn, appears to quickly decay into a solitonic vortex pair ($t = 15$ ms). This solitonic vortex pair then performs back-and-forth oscillations along the $z$ direction of the trap. It is crucial to note that, contrary to what was observed for the evolution of the initially stationary dark soliton stripe placed at $z = 0$ (see panel (a) of figure 5), the two solitonic vortices in this case remain *bound* as a pair for all times, in a way reminiscent of the vortex ring from which they emerged. The binding between these two solitonic vortices is provided by a narrow (weak) vortex ring-like vorticity structure that surrounds it. This binding vorticity is clearly appreciated in the light vorticity isocontours of the panel. It is worth pointing out that the process of decay from dark soliton stripes to vortex rings and solitonic vortices produces some surface waves in the condensate (see ripples at the periphery of the cloud's density in all 3D renderings) that also contain a small amount of vorticity that can be observed in some of the vorticity isocontours corresponding to low vorticity (see e.g. the light surfaces around $z = 0$ and 20 $\mu$m in panel (b) of figure 5 for $t = 200$ ms). These surface waves are also visible (additional faint lines) in the evolution of the integrated density in figure 4 (and also in figures 6, 8 and 10).

Let us now focus our attention on the collision of the localized structures we have been describing. In figure 6 we depict two examples of 'dark soliton stripe' collisions. The left panel shows a collision when a faster moving dark soliton stripe catches up with a slower moving one. The right panel shows a faster dark soliton stripe that bounces back from the edge of the condensate cloud and collides head-on with a slower moving dark soliton stripe. In these two examples the collisions of the dark soliton stripes seem to follow the known dynamics of interacting and colliding dark solitons. In that line, observing such collisions seems to suggest dynamics in close correspondence with the well-known integrable dynamics of dark-soliton collisions [8]. However, even in this innocent-looking case, the dynamics is considerably more elaborate in the present experimental setting. More specifically, after close inspection,

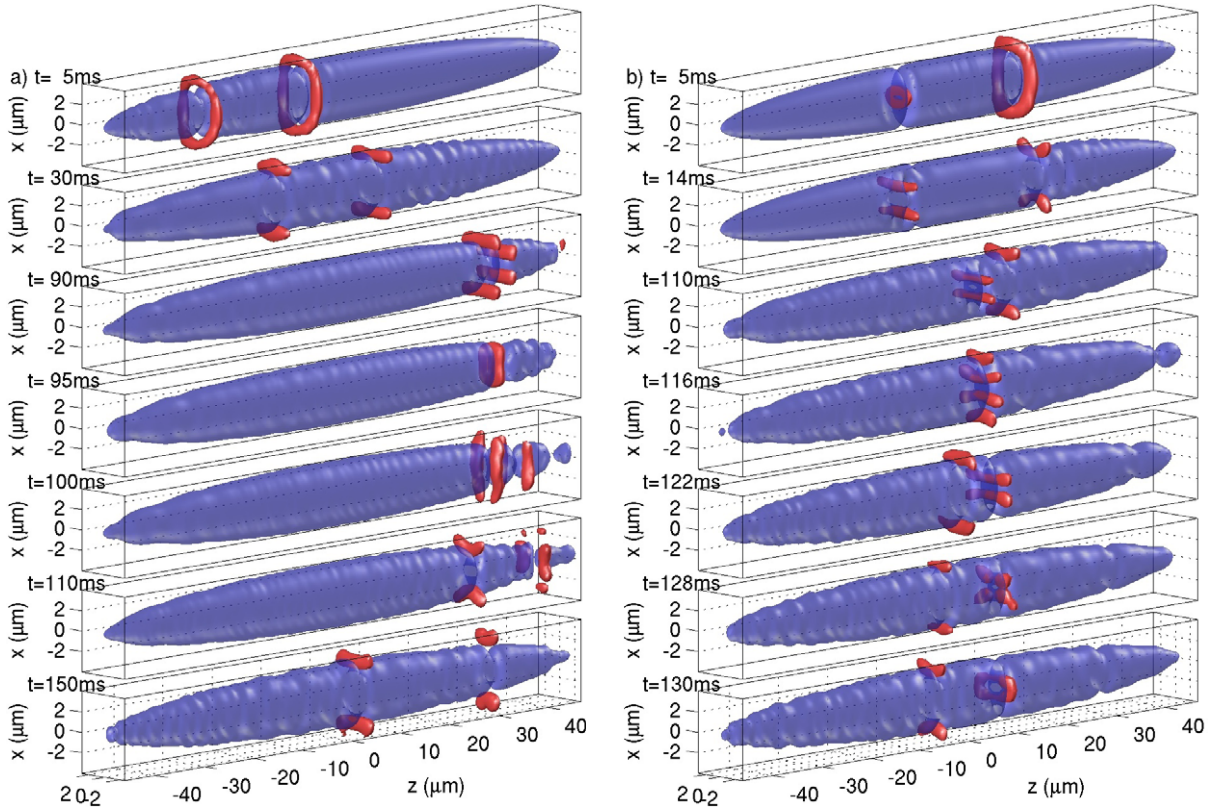


**Figure 7.** 3D renderings corresponding to the numerics shown in figure 6 with density and vorticity isocontours at 40 and 85%, respectively.

see corresponding 3D renderings depicted in figure 7, the dark soliton stripes are, in reality, identified as a pair of vortex rings ($t = 5$ ms) that subsequently appear as two pairs of solitonic vortices that oscillate inside the trap. In these two cases the solitonic vortex pairs interact *weakly* during collision. That is the 3D renderings of the condensates suggest that during the 'collision' event, the internal separation between vortex lines is different for the two solitonic vortices; as a result, the interaction during collision is relatively weak, despite the appearance of such an event in the integrated $(z, t)$-plots of figure 6. This type of relatively weak interaction, corresponding to seemingly elastic collisions of dark soliton stripes in the integrated density plots of figure 6, is a consequence of the relatively large difference of the respective speeds between the two solitonic vortex pairs as we now explain.

It is well known that the speed of a vortex ring decreases when its diameter increases [61]. Therefore, our solitonic vortex pairs (whose dynamics is strongly reminiscent of vortex rings) traveling at different speeds will have different inter vortex line separations and this separation will be larger for larger difference between their respective speeds. This is why two solitonic vortex pairs with relatively large difference between their speeds correspond to ones with relatively large difference in their internal separations which can consequently pass through each other with minimal interaction. This effect can be observed by comparing the two panels in figure 7: panel (b) corresponds to a larger difference between the speeds of the two solitonic vortex pairs and thus the interaction is weaker than the corresponding one of panel (a).

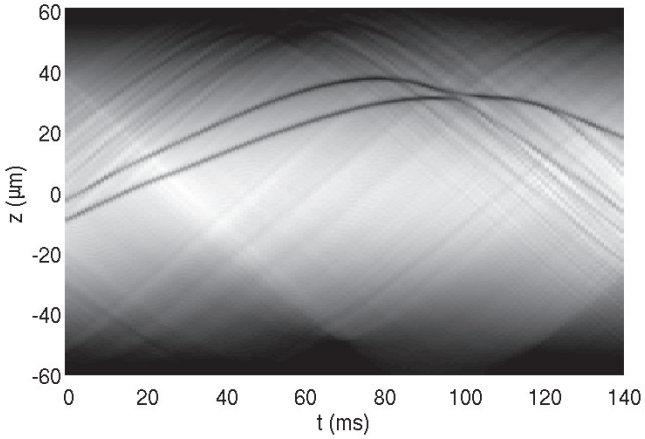


**Figure 8.** Numerical evolution of two chasing dark soliton stripes modeling conditions proximal to the experimental results shown in figure 2. As in figure 2, we show here the time evolution of the density integrated about the $x$ and $y$ directions.

Nonetheless, both of these examples can still be considered as weak interactions as the resulting 'collisions' seem practically elastic.

In contrast, when the two solitonic vortex pairs have similar velocities, the interaction is much more complex leading to unexpected behavior. As we show now, this unexpected behavior lies at the heart of what seems to be a merger of two dark soliton stripes in our experiment as shown in figure 2. Figure 8 is our numerical attempt to create conditions similar to the ones displayed by the experiment. In this case we start with two dark soliton stripes that give rise to two vortex rings which appear in the illustrated dynamical simulations in the form of solitonic vortex pairs whose velocities are relatively close. As it can be observed from figure 8, we obtain a qualitatively similar scenario as the one observed in our experiment: the two solitonic vortex pairs approach each other, after the outer one 'bounces back' from the edge of the cloud, and collide ($t = 100$ ms) resulting in one of the waves (the one closer to the center) becoming almost imperceptible and being sling shot away at a relatively large velocity. In figure 9 we depict the 3D renderings detailing the collision between these two solitonic vortices. As it is clear from the figure, the two solitonic vortex pairs interact very strongly because their internal separation is almost identical. This strong interaction is responsible for one of the solitonic vortex pairs being sling shot away at a faster speed, leaving behind what appears at $t = 112$ ms to clearly be a single vortex ring. Also, at the same time, this ejected pair is relegated to the periphery of the cloud in the $x$ and $y$ directions where the density is much weaker and so is its imprint in the integrated density plot of figure 8, resulting in a longitudinal observation of an apparent merger of two solitonic vortex pairs. This process is partially in line with the observation of [62] that intermediate collision velocities suffer the most inelasticity, yet, to the best of our understanding the latter work never observed numerically (or referred to experimental) scenaria as dramatic as the one above. This process is naturally suggestive of the fate of the experimental evolution depicted in figure 2 where the seemingly 'plastic' collision of two apparent dark soliton stripes (which, we essentially argue are really solitonic vortex pairs), at around $t \approx 100$ ms, seems to have one of the apparent dark soliton stripes to mysteriously disappear.

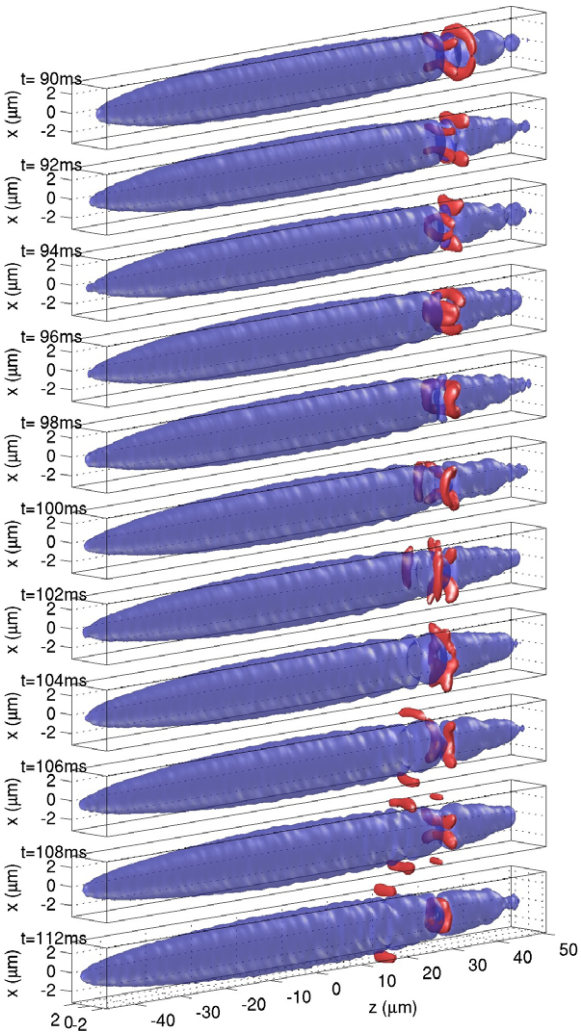


**Figure 9.** 3D renderings corresponding to the numerics shown in figure 8 depicting the sling shot effect suffered by one of the solitonic vortex pairs during collision. Density and vorticity isocontours at 40 and 85%, respectively.

Finally, motivated by the above example, we depict in figure 10 another extreme example of an apparently inelastic collision between dark soliton stripes. As it can be seen in the corresponding 3D renderings in figure 11, these are not true dark soliton stripes but rather interacting vortex rings/solitonic vortex pairs. In that context, the interactions instead of arising in regular intervals as in [20, 21], they instead appear to arise in intervals of increasing duration, leading to an expanding array of 'bubbles' (each spatio-temporal bubble amounting to a pair of collisions). Once again, resorting to the three-dimensionality of the original problem, we clearly observe the two solitonic vortices interacting. Then, their vortex character (as a manifestation of anisotropic quasi-two-dimensionality), given their same charge, enables the possibility of rotation of the vortices around each other. However, this rotation remains 'incomplete' due to its confined (anisotropic in $(x, y)$) nature. As the initial potential energy of interaction translates itself into rotational energy and partly gets emitted through phonon radiation, it makes the solitonic vortices gradually get grayer and grayer, hence more mobile within the least confined

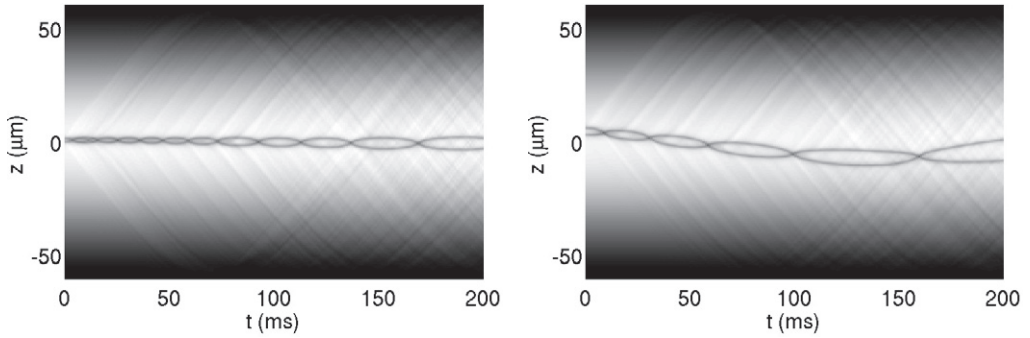


**Figure 10.** Evolution of two interacting seemingly dark soliton stripes (in reality, solitonic vortices). These panels depict seemingly interacting dark soliton stripes interacting in a highly uncharacteristic manner. These are really solitonic vortices instead of dark soliton stripes which are initially at rest. Left: solitonic vortices placed symmetrically about the center of the trap. Right: same configuration but slightly displaced in the $z$ direction. All panels depict the time evolution of the density integrated about the $x$ and $y$ directions.

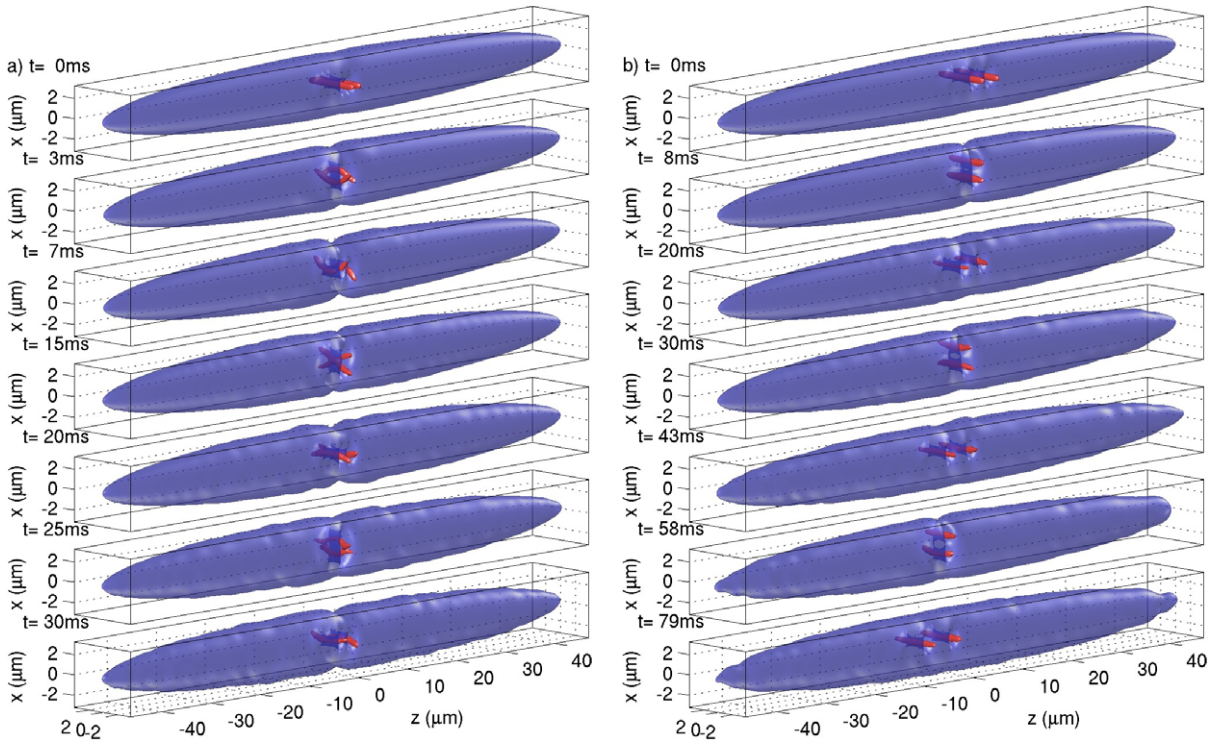


**Figure 11.** 3D renderings corresponding to the numerics shown in figure 10. Density and vorticity isocontours at 40 and 85%, respectively.

$z$-direction. The result of this gradually increased mobility is the more and more delayed repetition of their mutual interaction, which, in turn, is mirrored in the expanding bubbles in the $(z, t)$-plane.

## 4. Conclusions

In this paper, by comparing experimental and numerical results in anisotropically trapped Bose–Einstein condensates, we show that within the 'secret lives' of higher dimensional dark solitons, there is more than meets the eye in a quasi-1D inspection. We start by considering a set of numerical investigations with examples that exhibit either well-known dynamical phenomena (snaking instability) or simple and innocent-looking collisional events featuring apparently elastic interactions between dark soliton stripes. In each of these cases, we revealed that the true identity of the relevant states consisted of solitonic vortices and vortex rings. The hidden vortical nature of these higher dimensional structures opens the possibility for unexpected dynamics and interactions. In particular, we showcased an experimental realization that clearly displays the manifestation of this hidden property in a seemingly 'plastic' collision with the (apparent) merger of two dark soliton stripes, completely at odds with the quasi-1D, elastic particle character of these waves. Our numerical analogue of this experimental observation evidences a higher-dimensional complex dynamics involving strong interactions between two solitonic vortex pairs. There, the apparent merger was the result of a strong interaction between the waves whereby one of them was sling shot away.

Finally, in addition to this sling shot event, an example of expanding oscillation bubbles with longer times between collisions was presented and illustrated the vortical character of the solitonic vortex interactions. On the basis of these features, for our particular setting of trapping strengths, the projection in the $x$ direction seems to unveil the dynamics of dark soliton stripes since the $y$ direction is strong enough to arrest most dynamics and any instabilities across its length. Yet, the $x$ direction is weak enough to allow for the nucleation of solitonic vortices (vortex lines) aligned in the $y$ direction, as well as for the illustration of vortex ring type features. It is these extra structures, hidden in the $x$ direction, that induce the highly atypical behavior of the apparent dark soliton stripes, as observed in the $z$ direction.

Future experimental investigations within the regime under consideration here could employ simultaneous absorption imaging from two perpendicular directions—$x$ and $y$—which would allow for a better and unambiguous identification of the excitations. More generally, we believe that the present investigation illustrates the substantial value of potential further examination of interaction of quasi-1D structures in higher dimensional and especially in anisotropic geometries. The context of interaction of bright solitons [5] and even bright vortices in such a non-1D context that enables radial excitations is certainly worthwhile of further study. At the same time the study of solitonic vortices and vortex rings and the potential scenaria of their interaction [47] (as well as those of the interactions between different states or with more complex U- or S-shaped structures) in experimentally relevant settings certainly merits further examination and quantification, along lines similar to what has recently been done for dark solitons [20, 21] and also vortices [63, 64].

## Acknowledgments

We would like to thank S Stellmer, P Soltan-Panahi and S Dörscher for experimental support. PGK gratefully acknowledges support from the National Science Foundation under grants DMS-0806762 and CMMI-1000337, as well as from the Alexander von Humboldt Foundation, the Alexander S Onassis Public Benefit Foundation and the Binational Science Foundation. RCG gratefully acknowledges support from the National Science Foundation

under grant DMS-0806762. PS gratefully acknowledges financial support by the Deutsche Forschungsgemeinschaft under grant Schm885/26-1.

## References

[1] Pethick C J and Smith H 2008 *Bose–Einstein Condensation in Dilute Gases* 2nd edn (Cambridge: Cambridge University Press)
[2] Pitaevskii L P and Stringari S 2003 *Bose–Einstein Condensation* (Oxford: Oxford University Press)
[3] Strecker K E, Partridge G B, Truscott A G and Hulet R G 2002 *Nature* **417** 150
[4] Khaykovich L, Schreck F, Ferrari G, Bourdel T, Cubizolles J, Carr L D, Castin Y and Salomon C 2002 *Science* **296** 1290
[5] Cornish S L, Thompson S T and Wieman C E 2006 *Phys. Rev. Lett.* **96** 170401
[6] Eiermann B, Anker Th, Albiez M, Taglieber M, Treutlein P, Marzlin K-P and Oberthaler M K 2004 *Phys. Rev. Lett.* **92** 230401
[7] Kevrekidis P G, Frantzeskakis D J and Carretero-González R (ed) 2008 *Emergent Nonlinear Phenomena in Bose–Einstein Condensates: Theory and Experiment* (Berlin: Springer)
[8] Frantzeskakis D J 2010 *J. Phys. A: Math. Theor.* **43** 213001
[9] Fetter A L and Svidzinsky A A 2001 *J. Phys.: Condens. Matter* **13** R135
[10] Fetter A L 2009 *Rev. Mod. Phys.* **81** 647
[11] Brand J and Reinhardt W P 2001 *J. Phys. B: At. Mol. Opt. Phys.* **34** L113
[12] Komineas S 2007 *Eur. Phys. J. Spec. Top.* **147** 133
[13] Burger S, Bongs K, Dettmer S, Ertmer W, Sengstock K, Sanpera A, Shlyapnikov G V and Lewenstein M 1999 *Phys. Rev. Lett.* **83** 5198
[14] Denschlag J *et al* 2000 *Science* **287** 97
[15] Dutton Z, Budde M, Slowe C and Hau L V 2001 *Science* **293** 663
[16] Bongs K, Burger S, Dettmer S, Hellweg D, Arlt J, Ertmer W and Sengstock K 2001 *C. R. Acad. Sci., Paris* **2** 671
[17] Engels P and Atherton C 2007 *Phys. Rev. Lett.* **99** 160405
[18] Becker C, Stellmer S, Soltan-Panahi P, Dörscher S, Baumert M, Richter E-M, Kronjäger J, Bongs K and Sengstock K 2008 *Nature Phys.* **4** 496
[19] Stellmer S, Becker C, Soltan-Panahi P, Richter E-M, Dörscher S, Baumert M, Kronjäger J, Bongs K and Sengstock K 2008 *Phys. Rev. Lett.* **101** 120406
[20] Weller A, Ronzheimer J P, Gross C, Esteve J, Oberthaler M K, Frantzeskakis D J, Theocharis G and Kevrekidis P G 2008 *Phys. Rev. Lett.* **101** 130401
[21] Theocharis G, Weller A, Ronzheimer J P, Gross C, Oberthaler M K, Kevrekidis P G and Frantzeskakis D J 2010 *Phys. Rev.* A **81** 063604
[22] Shomroni I, Lahoud E, Levy S and Steinhauer J 2009 *Nature Phys.* **5** 193
[23] Matthews M R, Anderson B P, Haljan P C, Hall D S, Wieman C E and Cornell E A 1999 *Phys. Rev. Lett.* **83** 2498
[24] Williams J E and Holland M J 1999 *Nature* **401** 568
[25] Madison K W, Chevy F, Wohlleben W and Dalibard J 2000 *Phys. Rev. Lett.* **84** 806
[26] Recati A, Zambelli F and Stringari S 2001 *Phys. Rev. Lett.* **86** 377
[27] Sinha S and Castin Y 2001 *Phys. Rev. Lett.* **87** 190402
[28] Corro I, Scott R G and Martin A M 2009 *Phys. Rev.* A **80** 033609
[29] Madison K W, Chevy F, Bretin V and Dalibard J 2001 *Phys. Rev. Lett.* **86** 4443
[30] Raman C, Abo-Shaeer J R, Vogels J M, Xu K and Ketterle W 2001 *Phys. Rev. Lett.* **87** 210402
[31] Onofrio R, Raman C, Vogels J M, Abo-Shaeer J R, Chikkatur A P and Ketterle W 2000 *Phys. Rev. Lett.* **85** 2228
[32] Neely T W, Samson E C, Bradley A S, Davis M J and Anderson B P 2010 *Phys. Rev. Lett.* **104** 160401

[33] Scherer D R, Weiler C N, Neely T W and Anderson B P 2007 *Phys. Rev. Lett.* **98** 110402
[34] Weiler C N, Neely T W, Scherer D R, Bradley A S, Davis M J and Anderson B P 2008 *Nature* **455** 948
[35] Freilich D V, Bianchi D M, Kaufman A M, Langin T K and Hall D S 2010 *Science* **329** 1182
[36] Leanhardt A E, Görlitz A, Chikkatur A P, Kielpinski D, Shin Y, Pritchard D E and Ketterle W 2002 *Phys. Rev. Lett.* **89** 190403
Shin Y, Saba M, Vengalattore M, Pasquini T A, Sanner C, Leanhardt A E, Prentiss M, Pritchard D E and Ketterle W 2004 *Phys. Rev. Lett.* **93** 160406
[37] Komineas S and Papanicolaou N 2003 *Phys. Rev.* A **68** 043617
[38] Aftalion A and Danaila I 2003 *Phys. Rev.* A **68** 023603
[39] Komineas S, Cooper N R and Papanicolaou N 2005 *Phys. Rev.* A **72** 053624
[40] Simula T P 2011 *Phys. Rev.* A **84** 021603
[41] Donnelly R J 1991 *Quantized Vortices in Helium II* (Cambridge: Cambridge University Press)
[42] Rodrigues A S, Kevrekidis P G, Carretero-González R, Alexander T J, Frantzeskakis D J, Schmelcher P and Kivshar Yu S 2009 *Phys. Rev.* A **79** 043603
[43] Carretero-González R, Whitaker N, Kevrekidis P G and Frantzeskakis D J 2008 *Phys. Rev.* A **77** 023605
[44] Carretero-González R, Anderson B P, Kevrekidis P G, Frantzeskakis D J and Weiler C N 2008 *Phys. Rev.* A **77** 033625
[45] Ruostekoski J and Dutton Z 2005 *Phys. Rev.* A **72** 063626
[46] Sasaki K, Suzuki N and Saito H 2011 *Phys. Rev.* A **83** 033602
[47] Ginsberg N S, Brand J and Hau L V 2005 *Phys. Rev. Lett.* **94** 040403
[48] Feder D L, Pindzola M S, Collins L A, Schneider B I and Clark C W 2000 *Phys. Rev.* A **62** 053606
[49] Kuznetsov E A and Turitsyn S K 1988 1988 *Zh. Eksp. Teor. Fiz.* **94** 119
Kuznetsov E A and Turitsyn S K 1988 *Sov. Phys.—JETP* **67** 1583 (Engl. transl.)
[50] Kuznetsov E A and Rasmussen J J 1995 *Phys. Rev.* E **51** 4479
[51] Pelinovsky D E, Stepanyants Yu A and Kivshar Yu S 1995 *Phys. Rev.* E **51** 5016
[52] Tikhonenko V, Christou J, Luther-Davies B and Kivshar Yu S 1996 *Opt. Lett.* **21** 1129
[53] Mamaev A V, Saffman M and Zozulya A A 1996 *Phys. Rev. Lett.* **76** 2262
[54] Kivshar Yu S and Luther-Davies B 1998 *Phys. Rep.* **298** 81
[55] Anderson B P, Haljan P C, Regal C A, Feder D L, Collins L A, Clark C W and Cornell E A 2001 *Phys. Rev. Lett.* **86** 2926
[56] Brand J and Reinhardt W P 2002 *Phys. Rev.* A **65** 043612
[57] Muryshev A E, van Linden van, den Heuvell H B and Shlyapnikov G V 1999 *Phys. Rev.* A **60** R2665
[58] Kevrekidis P G, Theocharis G, Frantzeskakis D J and Trombettoni A 2004 *Phys. Rev.* A **70** 023602
[59] Kivshar Yu S and Pelinovsky D E 2000 *Phys. Rep.* **331** 117
[60] Kamchatnov A M and Korneev S V 2011 *Phys. Lett.* A **375** 2577
[61] Amit D and Gross E P 1966 *Phys. Rev.* **145** 130
Fetter A L 1966 *Phys. Rev.* **151** 100
Roberts P H and Grant J 1971 *J. Phys. A: Gen. Phys.* **4** 55
[62] Komineas S and Brand J 2005 *Phys. Rev. Lett.* **95** 110401
[63] Middelkamp S, Torres P J, Kevrekidis P G, Frantzeskakis D J, Carretero-González R, Schmelcher P, Freilich D V and Hall D S 2011 *Phys. Rev.* A **84** 011605
[64] Torres P J, Kevrekidis P G, Frantzeskakis D J, Carretero-González R, Schmelcher P and Hall D S 2011 *Phys. Lett.* A **375** 3044